AD-A117 392 ARMY ARMAMENT RESEARCH AND DEVELOPMENT COMMAND DOVER--ETC F/G 12/1
A MORE RATIONAL APPROACH TO THE STRESS ANALYSIS OF PROJECTILES.(U)
JUN 82 S C CHU, J STEINER

UNCLASSIFIED

NL

END
DATE FILMED
8-82
DTIC

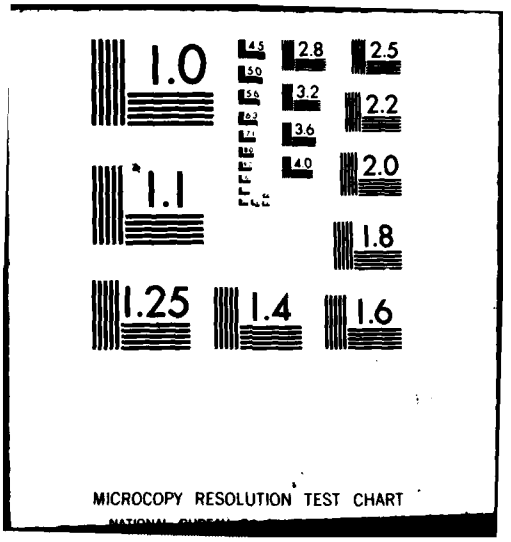
1.0
1.1
1.25
1.4
1.6
1.8
2.0
2.2
2.5
2.8
3.2
3.6
4.0
MICROCOPY RESOLUTION TEST CHART

18 JUN 1982

*CHU and STEINER

# A MORE RATIONAL APPROACH TO THE STRESS ANALYSIS OF PROJECTILES

*SHIH C. CHU, PhD
JAMES STEINER, MR.
TECHNOLOGY BR, ARMAMENT DIV, FC&SCWSL
US ARMY ARMAMENT RESEARCH AND DEVELOPMENT COMMAND
DOVER, NEW JERSEY 07801

## INTRODUCTION

Projectiles are traditionally analyzed and designed by using theory of elasticity, [1,2,3]. In this approach, the entire projectile body is considered to be loaded within the elastic region. However, under actual firing conditions, the equivalent stress in some region of the projectile is much greater than the yield strength of the projectile material. Hence, plastic flow will be encountered in the projectile body. The present trend in stress analysis of weapon and ammunition components is to take into account, in a more rigorous fashion, the complex phenomena of plastic flow. This is due to the necessity of designing for maximum stress to achieve an optimal design. In this investigation, a more rigorous nonlinear technique is developed in order to predict the inelastic deformation and stress distributions of a projectile subjected to actual firing conditions. Both nonlinear material response and geometric nonlinearity have been taken into consideration. Nonlinearity of material properties has been taken into account by use of theories of plasticity. Geometric nonlinearity has been considered by use of the finite element approach. A complete inelastic stress analysis of a 30 mm XM TP projectile has been conducted. The intent of this investigation is to identify potential design flaws and critical regions of the projectile under actual firing environment. A load history was defined which subjected the projectile to the loads at various points on the barrel travel curve. A peak pressure of 60,000 psi, peak acceleration of $4.8 \times 10^7$ in./sec$^2$ and a maximum spin of 6,355 rad/sec were considered.

## CONSTITUTIVE EQUATIONS

The primary objective of this investigation is to develop a more rational, nonlinear elastoplastic method for analyzing and designing a projectile to achieve in-bore structural integrity. The incremental stress-strain relations associated with the Von Mises yield criterion obeying the kinematic-hardening law for work-hardening materials will be used. The kinematic hardening law in the incremental theory of plasticity was originally proposed by Prager [4], for the deformation of isothermal solids. Later, Prager [5] extended these formulations to the nonisothermal condition for rigid work-hardening solids. Recently, Chu [6,7], expanded Prager's work for solids of more general deformation state. A brief outline of the constitutive equations used in the analysis is now given.

The total increment strain tensor, $d\varepsilon_{ij}$ is assumed to be the sum of elastic part, $d\varepsilon^e_{ij}$ , plastic part, $d\varepsilon^p_{ij}$, and the part of thermal strain, $d\varepsilon^T_{ij}$, i.e.

$$d\varepsilon_{ij} = d\varepsilon^e_{ij} + d\varepsilon^P_{ij} + d\varepsilon^T_{ij} \tag{1}$$

The elastic strain components $d\varepsilon^e_{ij}$ are related to the incremental stress components, $d\sigma_{ij}$, by

$$d\sigma_{ij} = D_{ijkl}d\varepsilon^e_{kl} = D_{ijkl}(d\varepsilon_{ij} - d\varepsilon^P_{kl} - \beta dT\delta_{kl}) \tag{2}$$

in which $\beta$ is the thermal expansion coefficient, dT, is the change in temperature, and $\delta_{kl}$ is Kronecker delta. For isotropic material, the 4th rank material tensor, $D_{ijkl}$ is defined by

$$D_{ijkl} = \frac{E}{1+\nu}\ \delta_{ik}\delta_{jk} + \frac{\nu E}{(1+\nu)(1-2\nu)}\ \delta_{ij}\delta_{kl} \tag{3}$$

where E is Young's modulus and $\nu$ is Poission's ratio of material.

On the basis of the Von Mises yield criterion with temperature-dependent yield strength of a material, the yield surface can be represented as:

$$f = \frac{1}{2}\ S_{ij}S_{ij} - \kappa^2(T) = 0 \tag{4}$$

where

$$S_{ij} = (\sigma_{ij} - \alpha_{ij}) - \frac{1}{3}\ (\sigma_{kk} - \alpha_{kk})\delta_{ij}; \qquad S_{mm} = 0 \tag{5}$$

$\alpha_{ij}$ is a tensor representing the total translation of the center of the initial yield surface, and $\kappa$ is related to the uniaxial yield stress $\kappa = \sigma_y(T)/\sqrt{3}$.

In addition to the yield condition, a constitutive relation between plastic strain increments, stress, and stress increments is required to describe the inelastic behavior of a material. The constitutive relation (flow rule) used in this investigation is based on Drucker's postulate for work-hardening material [8]. The flow rule is given as:

$$d\varepsilon^P_{ij} = d\lambda \frac{\partial f}{\partial \sigma_{ij}} \tag{6}$$

where $d\lambda$ is a positive scalar quantity. On the basis of Drucker's statement, this plastic strain increment tensor must lie on the outward normal to the yield surface at the instantaneous stress state.

Based upon Prager's kinematic-hardening rule [4,9] with Ziegler's modification [10], the increment of translation of the center of the yield surface is assumed to be directed along the radius vector connecting the center of the yielding surface to the instantaneous stress state, i.e.,

$$d\alpha_{ij} = (\sigma_{ij} - \alpha_{ij})d\mu; \quad d\mu > 0 \tag{7}$$

where $d\mu$ can be determined provided the stress point remains on the translated yield surface during plastic flow, i.e.,

$$d\mu = \frac{\dfrac{\partial f}{\partial \sigma_{kl}} d\sigma_{kl} + \dfrac{\partial f}{\partial T} dT}{(\sigma_{mn} - \alpha_{mn}) \dfrac{\partial f}{\partial \sigma_{mn}}} \tag{8}$$

During plastic loading, the consistency condition requires that

$$df = \frac{\partial f}{\partial \sigma_{ij}}(d\sigma_{ij} - Cd\varepsilon^P_{ij}) + \frac{\partial f}{\partial T} dT = 0 \tag{9}$$

The plastic strain vector $Cd\varepsilon^P_{ij}$ is considered as the projection of $d\sigma_{ij}$ (and thus of $d\alpha_{ij}$) on the exterior normal to the yield surface, where C is a material constant. Hence, for small incremental of stress and strain, one can readily find that

$$d\lambda = \frac{\frac{\partial f}{\partial \sigma_{ij}} d\sigma_{ij} + \frac{\partial f}{\partial T} dT}{\left(\frac{\partial f}{\partial \sigma_{mn}}\right)\left(\frac{\partial f}{\partial \sigma_{mn}}\right)} \tag{10}$$

Therefore, the flow rule becauses

$$d\varepsilon^{P}_{ij} = \frac{\frac{\partial f}{\partial \sigma_{ij}}}{C\left(\frac{\partial f}{\partial \sigma_{mn}}\right)\left(\frac{\partial f}{\partial \sigma_{mn}}\right)} \left(\frac{\partial f}{\partial \sigma_{kl}} d\sigma_{kl} + \frac{\partial f}{\partial T} dT\right) \tag{11}$$

If axisymmetric deformation is considered, with reference to the cylindrical coordinates (r, θ, z) the state is defined by the nonvanishing stress components $\{d\sigma\}^T = \langle d\sigma_r, d\sigma_\theta, d\sigma_z, d\tau_{rz} \rangle$ and strain components $\{d\varepsilon\}^T = \langle d\varepsilon_r, d\varepsilon_\theta, d\varepsilon_z, d\gamma_{rz} \rangle$. Then, the incremental stress-strain relations are found in the following matrix form:

$$\{d\sigma\} = [\bar{D}]\{d\varepsilon\} - \beta dT \{B\} \tag{12}$$

in which,

$$[\bar{D}] = \frac{\lambda}{\nu}\begin{bmatrix} 1-\nu & \nu & \nu & 0 \\ \nu & 1-\nu & \nu & 0 \\ \nu & \nu & 1-\nu & 0 \\ 0 & 0 & 0 & \frac{1-2\nu}{2} \end{bmatrix} - \eta_1 \cdot \begin{bmatrix} S_r^2 & S_r S_\theta & S_r S_z & S_r \tau_{rz} \\ S_\theta S_r & S^2_\theta & S_\theta S_z & S_\theta \tau_{rz} \\ S_z S_r & S_z S_\theta & S_z^2 & S_z \tau_{rz} \\ \tau_{rz} S_r & \tau_{rz} S_\theta & \tau_{rz} S_z & \tau_{rz}^2 \end{bmatrix} \tag{13}$$

$$\{B\} = \frac{E}{1-2\nu}\begin{Bmatrix} 1 \\ 1 \\ 1 \\ 0 \end{Bmatrix} - \frac{\eta_2}{\beta} \cdot \frac{\partial \kappa}{\partial T} \begin{Bmatrix} S_r \\ S_\theta \\ S_z \\ \tau_{rz} \end{Bmatrix} \tag{14}$$

$$\lambda = \frac{E\nu}{(1+\nu)(1-2\nu)} \tag{15}$$

$$\eta_1 = \frac{1}{g} \left(\frac{E}{1+\nu}\right)^2 \tag{16}$$

$$\eta_2 = \frac{2\kappa}{g} \cdot \frac{E}{1+\nu} \quad \text{and,} \tag{17}$$

$$g = 2\kappa^2 \cdot \left(\frac{E}{1+\nu} + C\right) \tag{18}$$

## METHOD OF SOLUTION

The projectile and all loading acting on the projectile are considered as axisymmetric. A cylindrical coordinate system (r, θ, z) is used in this analysis. By the assumption of axial symmetry, all variables are independent of angle θ, consequently, all derivatives, with respect to θ vanish. The displacement $u_\theta$, and the shear stresses $\tau_{r\theta}$ and $\tau_{\theta z}$ vanish.

Due to the complexity of the geometry of a projectile and nonlinear material behavior, the finite element method [11,12] was used to conduct the stress analysis. The analytical approach used in this investigation is the incremental loading technique, wherein at each step of loading a new stiffness matrix is formulated, in terms of the finite element model, and solved for incremental deformations, stresses, and strains.

To perform a finite element stress analysis, the cross section of a projectile is divided into a large number of small triangular and quadrilateral elements as shown in Figure 1. Only a few nodal points on the boundary need be specified, the remaining nodal points are obtained from an automatic mesh generating computer program. The grid was partitioned to place a finer grid at those areas of the body that are expected to undergo large stress.

## PROJECTILE CONFIGURATION AND MATERIAL PROPERTIES

The outline of a 30 mm XM TP projectile is shown in Figure 2. The projectile is made of three distinct parts with three different materials as shown in Figure 2 (the projectile body, nose cap, and rotating band are made of 1018 steel, aluminum, and gilding metal, respectively). The material properties are given below:

| Material | Poisson's Ratio | Young's Modulus (psi) | Yielding Stress (psi) | Ultimate Stress (psi) | Density lb/in.$^3$ |
|---|---|---|---|---|---|
| Steel | .29 | $29\times10^6$ | 88,500 | 90,000 | .280 |
| Aluminum | .33 | $10\times10^6$ | 77,000 | 80,000 | .101 |
| Gilding Metal | .33 | $17\times10^6$ | 40,000 | 48,000 | .317 |

The stress-strain relations of those materials are shown in Figure 3.

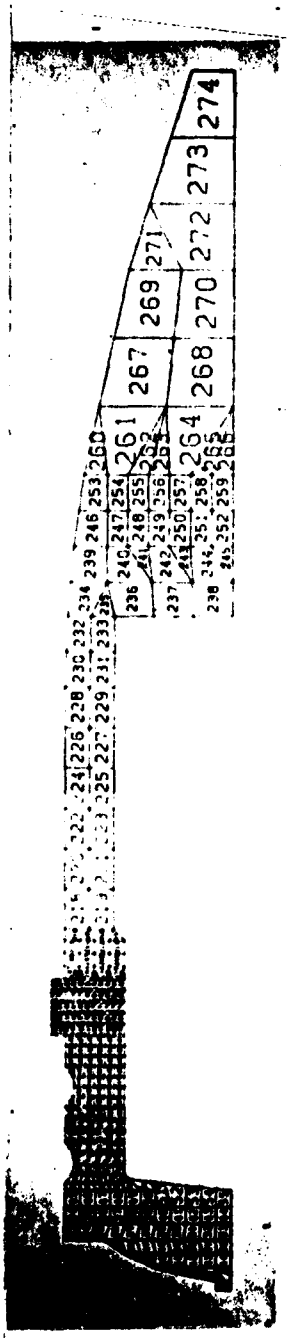

Figure 1. Finite Element Presentation of a Projectile

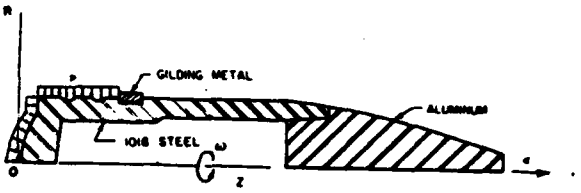


Figure 2. Projectile Configuration

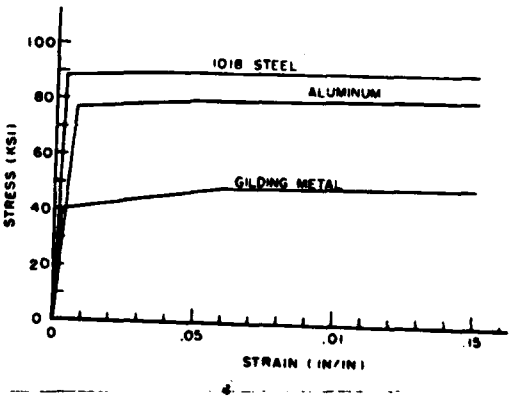


Figure 3. Stress-Strain Relation for Projectile Materials

## LOADING CONDITIONS

The loads considered in this investigation simulating the environment in the gun barrel during firing. The loading consisted of four types: (1) propellant gas pressure, (2) setback force due to acceleration, (3) rotational velocity due to the spin of projectile, and (4) forced displacement of the rotating band. The maximum value of these four types of loadings are given by, $P_{max}$ = 60,000 psi, $a_{max}$ = $4.8 \times 10^7$ in./sec$^2$, $\omega_{max}$ = 6,335 rad/sec, and $\Delta_{max}$ = -0.008 inches for gas pressure, acceleration, spin rate, and radial displacement, respectively. The frictional shear forces between the band and the barrel were neglected in this investigation. The loads were applied in incremental fashion with the relative magnitudes at each load point simulated the physical interdependence of the loads at different times during the interior ballistic cycle. The detailed loading history is given in Figure 4.

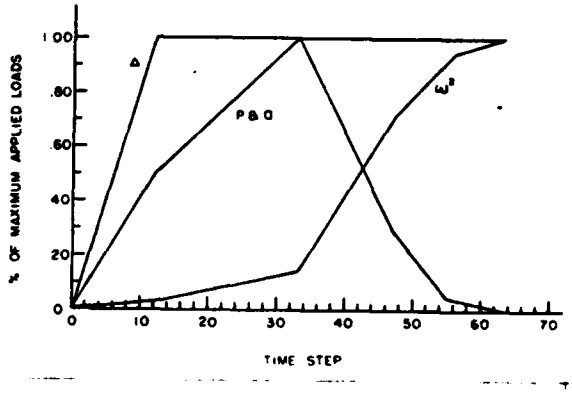


Figure 4. Loading History

## COMPUTATIONAL RESULTS

For each incremental loading, the stresses and strains of each element and the displacement of each nodal point were calculated. The plastic flow has been initiated within element 186 of the gilding metal at the end of the first step of loading. Based upon the Von Mises yield criteria, the equivalent stress for each element was calculated. At the end of the first step of loading, the maximum equivalent stress ($\sigma_e$) in the projectile body is 69,900 psi which is lower than yielding strength of 1018 steel (element 174), and in the gilding metal portion is 40,000 psi (element 186), which is equal to the yield strength of the gilding material.

The computation results presented in this section are based upon the following three major loading steps (shown in Figure 4):

1) At the end of the 12th step ($\Delta$=1.0, p=0.5, a=0.5, and $\omega^2$=0.036) while the forced displacement reeaches the maximum in the rotating band.

2) At the end of the 33rd step, ($\Delta$=1.0, p=1.0, a=1.0, and $\omega^2$=0.14) while both propellant gas pressure and setback force reach the peak.

3) At the end of the 63rd step ($\Delta$=1.0, p=0, a=0, and $\omega^2$ = 1.0), while the spin rate reaches the maximum at the muzzle end of the tube.

The plastic range in the projectile under the above three loading conditions is shown in Figure 5, 6, and 7, as indicated by the shaded area.

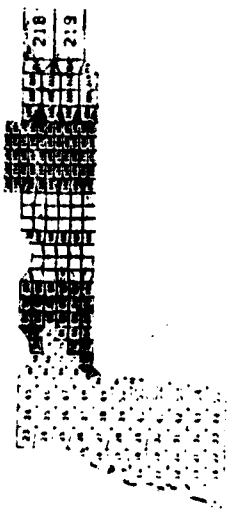


Figure 5. Plastic Zone in the Projectile at Loading Condition: $\Delta$=1.00, p=0.50, a=0.50 and $\omega^2$=.036

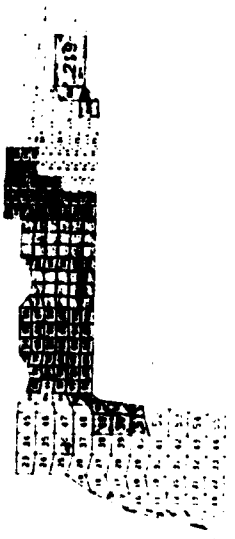


Figure 6. Plastic Zone in the Projectile at Loading Condition: $\Delta$=1.00, p=1,00, a=1.00 and $\omega^2$=0.14

*CHU and STEINER

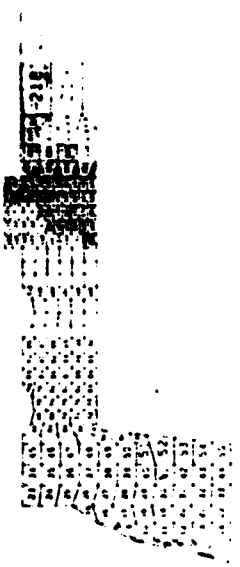

Figure 7. Plastic Zone in the Projectile at Loading Condition: $\Delta$=1.00, p=0.0, a=0.0 and $\omega^2$=1.00

The maximum plastic strains encountered in the gilding metal (element 186) is 0.027 in./in., and in the projectile is 0.025 in./in. (element 163) at the end of the 12th loading step, while the maximum radial displacement took place in the rotating band. The maximum plastic strains were increased to 0.0294 in./in. (element 186) in the gilding metal and to 0.0254 in./in. (element 163) in the projectile body, while both gas pressure and setback force reached the peak. When projectile reached the muzzle end the maximum plastic strains are 0.0294 in./in. and 0.0258 in./in. encountered in the elements 186 and 163, respectively. During the entire loading process the change of maximum plastic strain is small. The location of plastic zones under different loading conditions is important to the projectile design.

The equivalent stress along the length of the inner surface elements of the projectile is shown in Figure 8. The maximum equivalent stress reaches 88,800 psi, which is greater than the yielding strength ($\sigma_y$ = 88,500 psi) and smaller than the ultimate strength ($\sigma_u$ = 90,000 psi) of the projectile material. If the investigation was based on elastic analysis, the maximum equivalent stress could reach a value which would be much higher than the ultimate strength of the projectile material. This is the reason that our inelastic analysis technique be developed, since a more rigorous stress analysis can only be obtained by using nonlinear theories of plasticity as developed in this investigation.

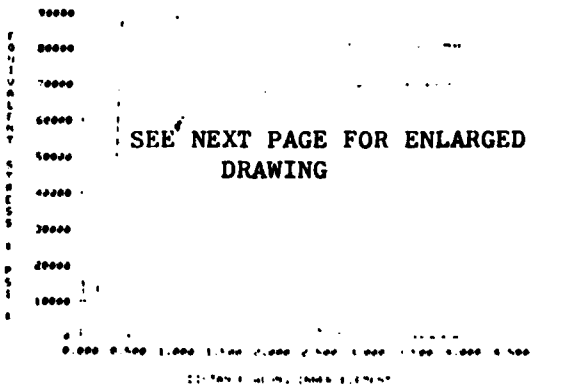


See Next Page for Enlarged Scale

Figure 8. Equivalent Stress in the Inner Elements of the Projectile.

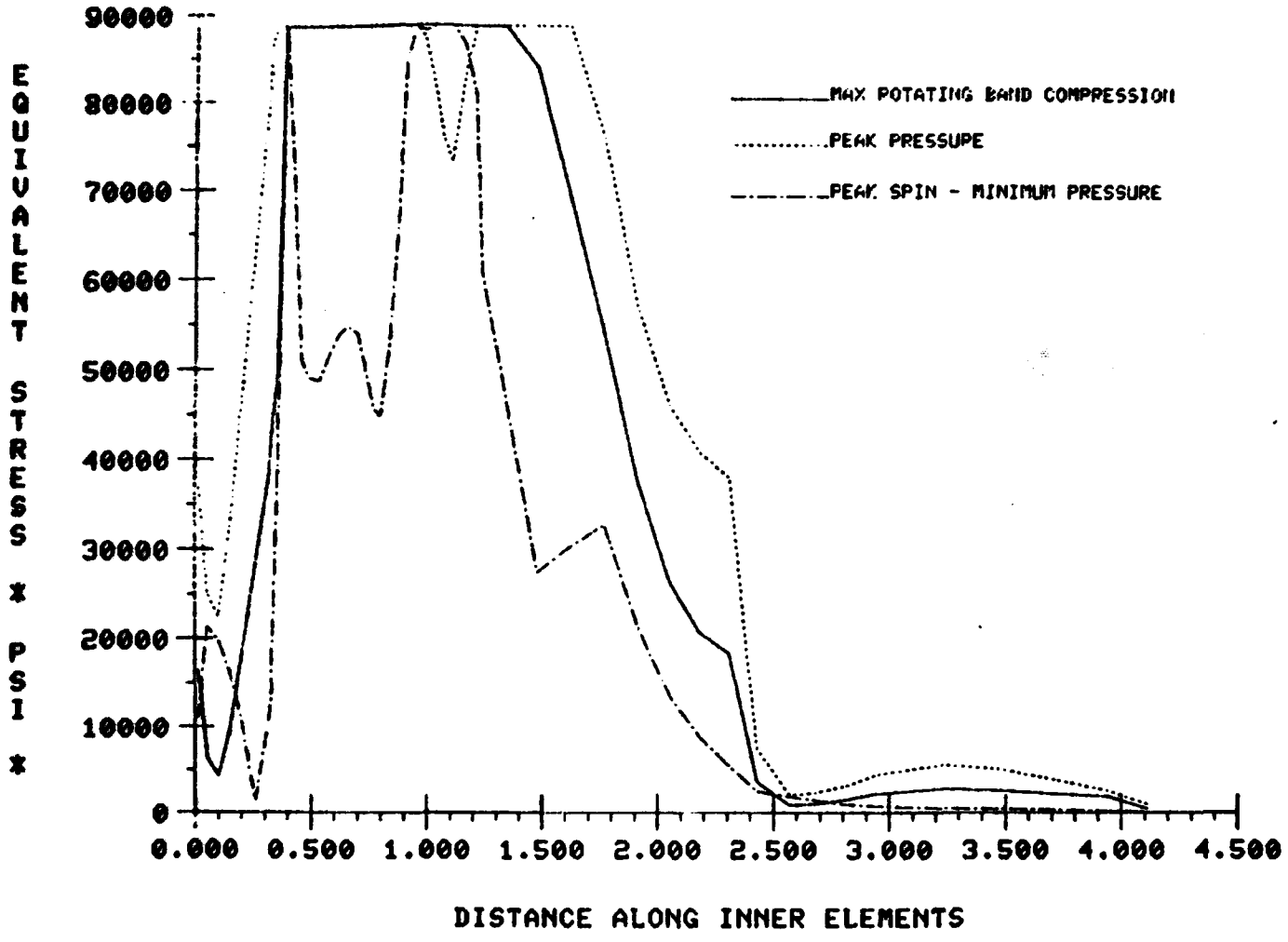


Figure 8 . Equivalent Stress in the Inner Elements of the Projectile.

The equivalent stress distribution in the projectile of high stressed region at peak pressure and setback is shown in Figure 9. It is clearly indicated that the critical region is located from the rotating band to the inside wall of projectile base.

The deformed grids under different loading conditions are shown in Figures 10, 11, and 12. The deformations shown in these Figures are the deformations enlarged 10 times in magnitude.

Figure 9. Equivalent Stress (KSI) Distribution in the Critical Region of the Projectile at Loading Condition: $\Delta$=1.0, p=1.0, a=1.0 and $\omega^2$=0.14

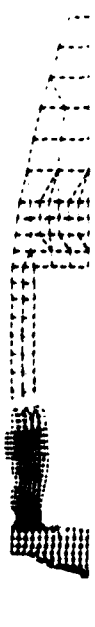

Figure 10. Deformed Grid Mesh Under Loading Condition: $\Delta$=1.0, p=0.5, a=0.5 and $\omega^2$=0.036

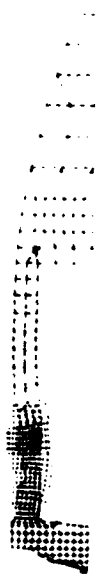

Figure 11. Deformed Grid Mesh Under Loading Condition: $\Delta$=1.0, p=1.0, a=1.0 and $\omega^2$=0.14

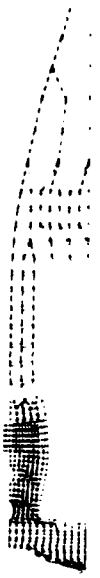

Figure 12. Deformed Grid Mesh Under Loading Condition: $\Delta$=1.0, p=0, a=0 and $\omega^2$=1.0

## CONCLUSIONS

On the basis of Drucker's flow rule of plasticity, the Von Mises flow criterion, and the strain-hardening and compressibility properties of a material, a more rational rigorous nonlinear elastoplastic analytic method has been develped for analyzing and designing a projectile subjected to actual complicated firing conditions. In constrast to the traditional designing and analyzing techniques (theories of elasticity), the complex phenomenal plastic flow in the projectile has been taken into account.

This is due to the necessity of designing for maximum stress to achieve an optimal design for reducing component weight. Both nonlinear material response and geometric nonlinearity have been taken into consideration. Nonlinearity of material properties has taken into account by use theories of platicity. Geometric nonlinearly has been considered by use the finite element technique. An incremental loading procedure has been used to consider the actual firing environment of a gun. The complete loading history which includes propellant gas pressure, setback force, and spin rate of a projectile was defined as function of time.

The critical region is located in the region between rotating band and projectile base. In this region the equivalent stress in general is above the yield strength of material, however, it is below ultimate strength of the material. The plastic strain has taken place in the reigon, however, maximum equivalent plastic-strain at inner surface is below 0.03 in./in., which is relatively small.

Based upon our investigation the plastic zone in the projectile has been identified and accurately located for each incremental of loading which simulating the actual fire environment in a gun. The developed technique will provide a more rigorous stress analysis tool for projectile design. The potential design flaws and critical regions of a projectile can be identified before the projectile is being made and tested.

## REFERENCES

1. DePhillipo, T.E., and Booth, A.W., "Mathematical Model for Determining Stresses in Projectile Bodies," Report R-1939, Frankford Arsenal Oct 1969.

2. Mechanical Engineering Department, New York University, "Principal and Combined Sresses of the Shell, HE 155 mm M197," Picatinny Arsenal Report U38115.

3. Elder, A.S., Burns, B.P., and Hurban, J.M., "Stress Analysis of 175 mm Projectile, HE M437, BRL Memorandum Report 2113.

4. Prager, W., "The Theory of Plasticity: A Survey of Recent Achievement (Hames Clayton Lecture)," Proc. Inst. Mech. Eng. 69 (1955).

5. Prager, W., "Nonisothermal Plastic Deformation," Proc. Koni, Ned. Akad., Van Weton, Series B, 61, NO (3), 1958.

6. Chu, S.C., "Nonisothermal Elastoplastic Deformation of Work-Hardening Solids," Paper presented at Joint ASME/ASCE Mechanics Conference, University of Colorado, 22-24 June 1981.

7. Chu, S.C., "An Incremental Appraoch to Nonisothermal Elastic-Plastic Deformation." Proc. 27th Conference of Army Mathematicians, 1981.

8. Drucker, D.C., "A More Fundamental Approach to Plastic Stress-Strain Relations," Proc. 1st U.S. National Congress Applied Mechanics, New York, 1952.

9. Prager, W., "A New Method of Analyzing Stresses and Strains in Work-Hardening Plastic Solids," Journal App. Mech. Vol. 23, 1956.

10. Ziegler, H., "A Modification of Prager's Hardening Rule," Quarterly of Appl. Math Vol. 17, 1959.

11. Zienkiewicz, O.C., "The Finite Element Method in Engineering Science." McGraw-Hill, 1971.

12. Marcal, P.V. and King, I.P., "Elastic-Plastic Analysis of Two-Dimensional Stress Systems by the Finite Element Method," Inter. J. Mech., Vol. 9, No. 3, 1967.